



ARTICLE

Electrochemical synthesis of three-dimensional flower-like Ni/Co–BTC bimetallic organic framework as heterogeneous catalyst for solvent-free and green synthesis of substituted chromeno[4,3-*b*]quinolones

Mohammad Hosein Sayahi¹ | Matineh Ghomi¹ | Samir M. Hamad² |
Mohammad Reza Ganjali^{3,4} | Mustafa Aghazadeh³ | Mohammad Mahdavi⁵ |
Saeed Bahadorikhalili⁶

¹Department of Chemistry, Payame Noor University (PNU), Tehran, Iran

²Scientific Research Center, Soran University, Soran, Iraq

³Center of Excellence in Electrochemistry, School of Chemistry, College of Science, University of Tehran, Tehran, Iran

⁴Biosensor Research Center, Endocrinology and Metabolism Molecular–Cellular Sciences Institute, Tehran University of Medical Sciences, Tehran, Iran

⁵Endocrinology and Metabolism Research Center, Endocrinology and Metabolism Clinical Sciences Institute, Tehran University of Medical Sciences, Tehran, Iran

⁶School of Chemistry, College of Science, University of Tehran, Tehran, Iran

Correspondence

Mohammad Hosein Sayahi, Department of Chemistry, Payame Noor University (PNU), P.O. Box 19395–3697, Tehran, Iran.

Email: sayahymh@pnu.ac.ir

Saeed Bahadorikhalili, School of Chemistry, College of Science, University of Tehran, Tehran, Iran.

Email: saeed.bahadorikhalili@khayam.ut.ac.ir

Funding information

University Research Council, Payame Noor University

Abstract

In this research, a new flower-like Ni_{0.77}/Co_{0.23}–benzene–1,3,5–tricarboxylate (BTC) bimetallic organic framework (Ni/Co–BTC BMOF) is synthesized via the cathodic electrosynthesis (CE) method, based on nickel and cobalt metals and BTC linker. The synthesized BMOF is characterized by several methods, including Fourier transform infrared spectroscopy (FT-IR), powder X-ray diffraction (PXRD), field emission scanning electron microscopy (FE-SEM), and energy dispersive X-ray analysis (EDX). The catalytic activity of the resulting Ni/Co is evaluated in a one-pot four-component reaction of dimedone, aromatic aldehyde, 4-hydroxycoumarin, and ammonium acetate for the synthesis of chromeno[4,3-*b*]quinolone derivatives under solvent-free condition. The Ni/Co–BTC BMOF catalyst showed very good activity in the tested reaction, and a wide scope of starting materials gave the desired products in high isolated yields in the presence of the Ni/Co–BTC BMOF catalyst. The recovery of Ni/Co BMOF was achieved by a centrifuge, and it was reused at least six times without any significant decrease in catalytic activity.

KEYWORDS

chromeno[4,3-*b*]quinolone, electrochemical synthesis, flower-like Ni/Co–BTC bimetallic organic framework, MOF catalyst, multicomponent reaction

1 | INTRODUCTION

Metal–organic frameworks (MOFs) are known as a new class of nanoporous crystalline solids. They comprise metal cations/clusters and organic linkers, which generate crystals with three-dimensional (3D) structures via self-assembly.^[1–3] Up to now, various chemical-based methods have been adopted to fabricate nano-sized MOFs, which include sonochemical,^[4,5] microwave-assisted,^[6,7] coordination modulation,^[8,9] solvothermal,^[10,11] microemulsion,^[12,13] hydrothermal, and template methods^[14] and electrochemical synthesis.^[15–18] Due to the easy synthesis process of MOFs and their remarkable properties, they have attracted interest in many different fields such as catalysis, sensors, gas storage, drug delivery, separation, and optics.^[19–23]

Recent research has focused on the potential of the synthesis of bimetallic MOFs (BMOFs) as a new type of MOFs to enhance framework stability, gas sorption, and catalytic activity and magnetic and luminescence properties.^[24–28] BMOFs include two different metal ions as a reactant with a ligand during the synthesis process, which leads to the pure phase of MOFs.^[21] Among different reported processes for the synthesis of BMOFs, the cathodic electrosynthesis (CE) method, based on the cathodic electrodeposition procedure, has attracted attention due to the efficient and controllable synthesis of MOF nanostructures.^[29] Through an electrochemical route, cathodic electrodeposition via base generation onto the cathode surface is a simple and inexpensive technique for nanostructured materials.^[30–33]

As BMOFs have catalytic centers and can be easily recycled and reused several times, they have been interestingly applied in catalytic processes.^[34–39] The catalytic effects of many BMOFs have been previously reported in different fields, including multicomponent reactions,^[39] photocatalytic performance,^[40] coupling,^[41,42] and oxidative degradation reactions.^[43] In addition, the synthesis of 2,4-disubstituted quinoline,^[44] cyclohexenones,^[45] functionalized dihydro-2-oxopyrroles,^[46] and Suzuki Miyaura cross-coupling^[47] has been made possible by BMOFs.

Here, the CE method was applied for the synthesis of Ni_{0.77}/Co_{0.23}-BTC BMOF from nickel nitrate, cobalt nitrate, and benzene-1,3,5-tricarboxylate (BTC). In this method, electrochemical generation of base anions (OH⁻) was achieved by the reduction of pro-base species like water molecules. The OH⁻ anions cause in situ deprotonation of the ligand and the deposition of nano-sized MOFs onto the cathode.^[48] The prepared Ni_{0.77}/Co_{0.23}-BTC BMOF was characterized by various techniques, including powder X-ray diffraction (PXRD), Fourier transform infrared spectroscopy (FT-IR), field

emission scanning electron microscopy (FE-SEM) and energy dispersive X-ray analysis (EDX), and was used as a heterogeneous catalyst for the one-pot and solvent-free synthesis of chromeno[4,3-*b*]quinolone via four-component reaction of dimedone, aromatic aldehyde, 4-hydroxycoumarin, and ammonium acetate at room temperature. The general route of this proposed research is illustrated in Scheme 1.

2 | RESULTS AND DISCUSSIONS

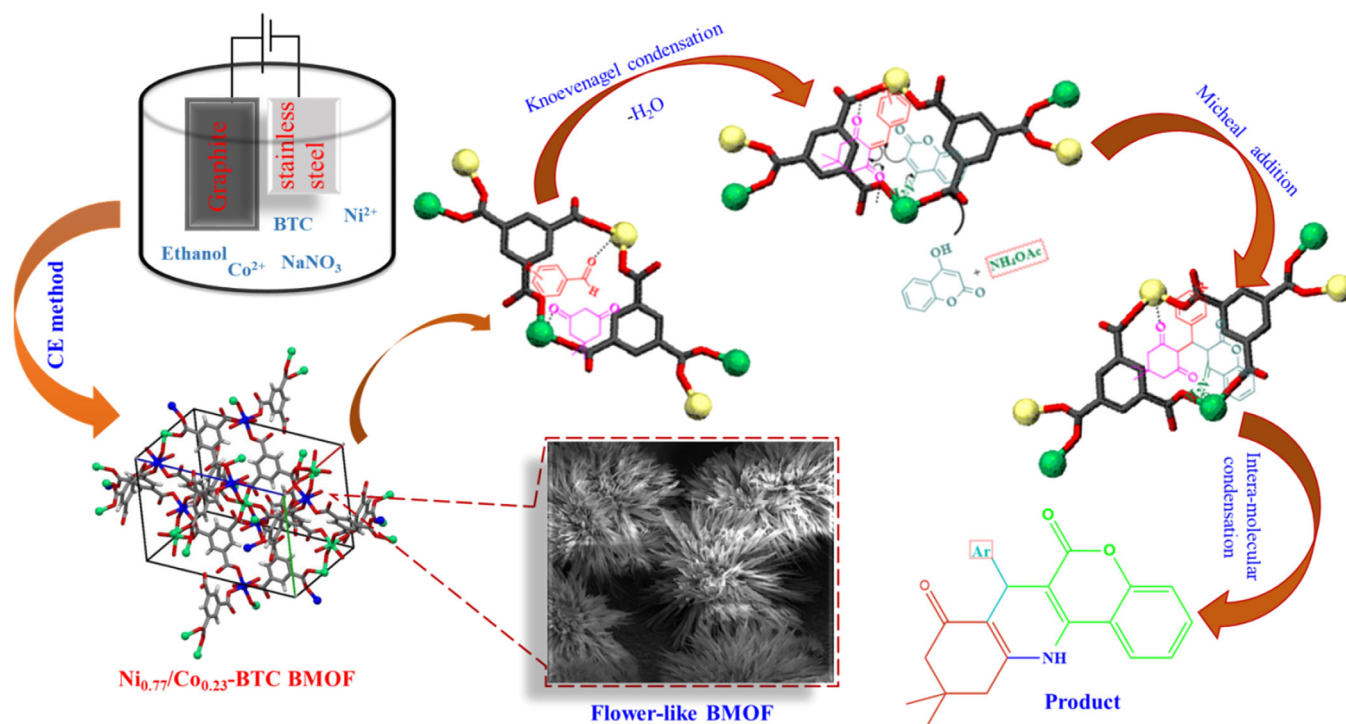
2.1 | Morphology, characterization, and sensing strategy

In order to ensure the synthesis of Ni_{0.77}/Co_{0.23}-BTC BMOF, several characterization methods were applied. The morphology and characterization of Ni_{0.77}/Co_{0.23}-BTC BMOF was obtained through various techniques such as XRD, FT-IR, FE-SEM, and EDS.

Figure 1a shows the XRD pattern of Ni_{0.77}/Co_{0.23}-BTC BMOF. The main observed diffraction peaks in this pattern are easily indexed to the crystal planes of [Ni₃(BTC)₂]. Furthermore, this pattern is identical to the pattern reported for Ni/Co-MOF in the literature.^[49,50] In addition, the XRD result is in good agreement with the single-crystal data of [M₃(BTC)₂ · 12H₂O] (M = Ni, Co) with CCDC number of 1274034. It should be noted that no impurity diffractions were observed in the XRD patterns. These observations indicate the pure crystalline nature of the synthesized BMOF.

The FT-IR spectrum of the sample is shown in Figure 1b. The bands at 3,440 cm⁻¹ and 3,108 cm⁻¹ are caused by the stretching vibration of water molecules, confirming the existence of coordinated H₂O molecules within the structure. The strong absorption bands at 1,648, 1,606, 1,546, 1,435, and 1,373 cm⁻¹ were assigned to the asymmetric and symmetric stretching modes of the coordinated (–COO⁻) group.^[51,52] It should be noted that, after doping of Co ions, the band at 1,648 cm⁻¹ appeared in Ni_{0.77}/Co_{0.23}-BTC BMOF, indicating that the Co²⁺ ions are successfully doped in the structure of the BMOF, and therefore, the surrounding environment of –COO⁻ group has been changed. The absence of absorption bands from 1,730 cm⁻¹ to 1,690 cm⁻¹ associated with the –COOH is indicative of the deprotonation of H₃BTC upon its contact with metal ions.^[49,50]

Surface morphology (i.e., FE-SEM images) for the fabricated Ni_{0.77}/Co_{0.23}-BTC BMOF is given in Figure 2a,b. 3D flower-like blocks are observed for the deposited Ni_{0.77}/Co_{0.23}-BTC BMOF powder (Figure 2a). Each observed 3D binding block is composed of many leaf-shaped nanoscale rods (Figure 2b).



SCHEME 1 The general route of this proposed research

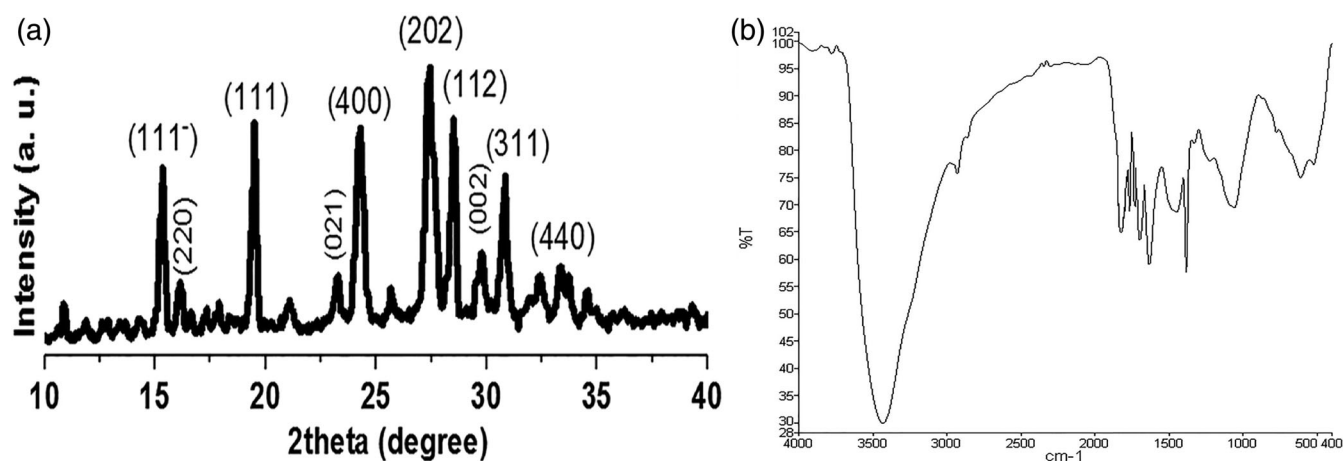


FIGURE 1 (a) XRD pattern and (b) FT-IR spectrum of $\text{Ni}_{0.77}/\text{Co}_{0.23}$ -BTC BMOF

The elemental analysis profile is also presented in Figure 2c. For the fabricated $\text{Ni}_{0.77}/\text{Co}_{0.23}$ -BTC BMOF sample, the elements of carbon, oxygen, nickel, and cobalt are detected in its chemical composition. The EDS result proves the successful synthesis of a bimetallic structure by the presence of both nickel and cobalt in the structure of the BMOF. The weight percentages of C, O, Co, and Ni are 36.04wt%, 43.53wt%, 4.59wt%, and 15.48wt%, respectively. The carbon and oxygen percentages confirmed the BTC content of the fabricated BMOF. The nickel and cobalt

percentages also demonstrated the bimetallic composition of the electro synthesized $\text{Ni}_{0.77}/\text{Co}_{0.23}$ -BTC BMOF.

In order to study the surface area and the pore size of $\text{Ni}_{0.77}/\text{Co}_{0.23}$ -BTC BMOF, BET analysis was applied. The Brunauer–Emmett–Teller (BET) and nitrogen adsorption–desorption results are presented in Table 1. It could be observed that $\text{Ni}_{0.77}/\text{Co}_{0.23}$ -BTC has a high surface area of $721.73 \text{ m}^2/\text{g}$. In addition, the pore width and pore volume of the synthesized BMOF are 3.11 nm and $0.69 \text{ cm}^3/\text{g}$, respectively.

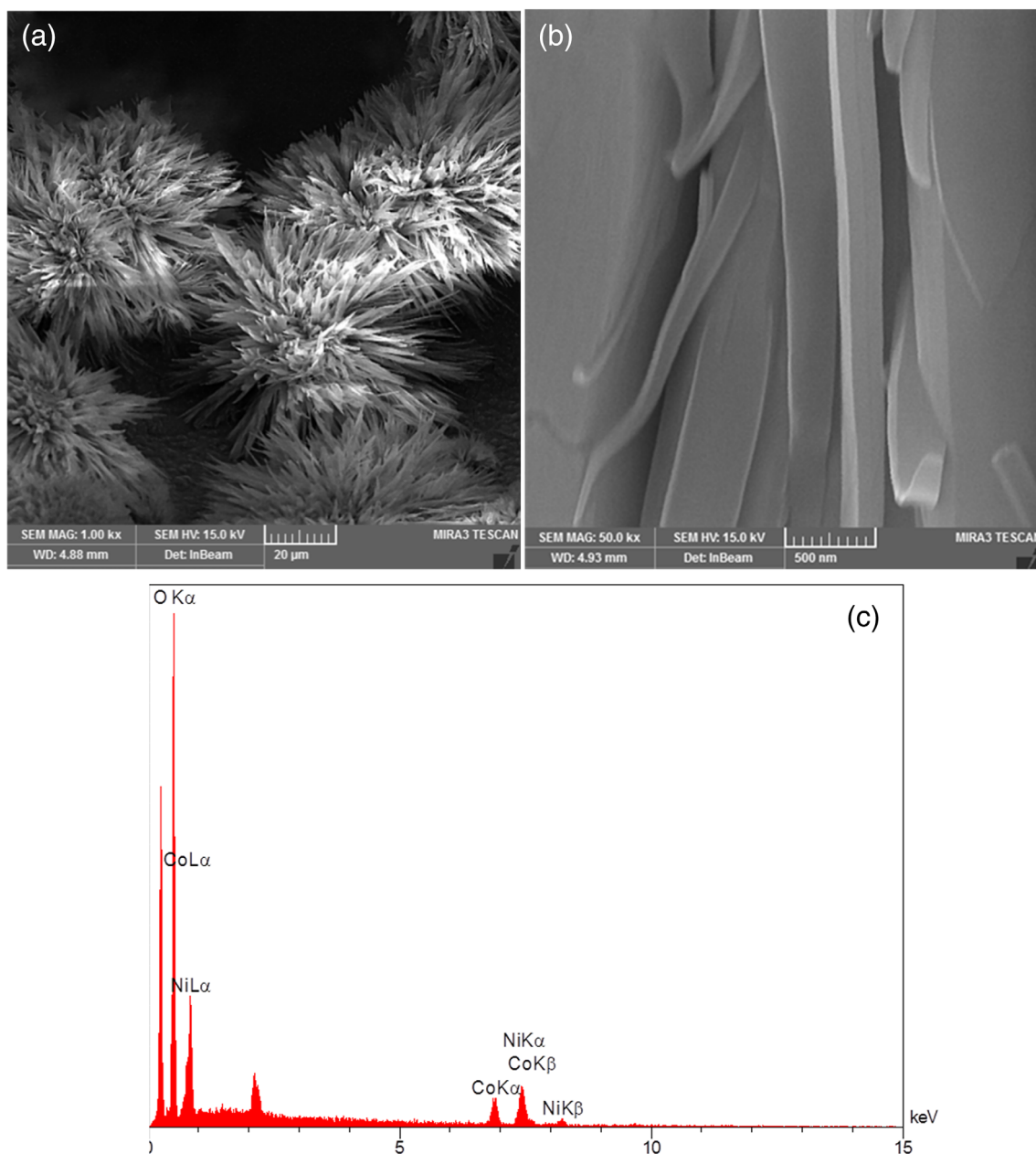


FIGURE 2 (a) 3D image of flower-like blocks of $\text{Ni}_{0.77}/\text{Co}_{0.23}$ -BTC BMOF, (b) 3D and leaf-shaped image of each block, and (c) EDAX analysis of $\text{Ni}_{0.77}/\text{Co}_{0.23}$ -BTC BMOF

TABLE 1 Surface area and pore size results of $\text{Ni}_{0.77}/\text{Co}_{0.23}$ -BTC BMOF

| | |
|--|--------|
| Surface area (m^2/g) | 721.73 |
| Pore width (nm) | 3.11 |
| Pore volume (cm^3/g) | 0.69 |

2.2 | Catalytic study

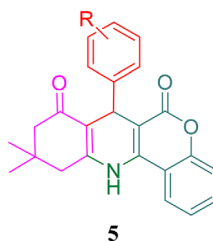
The catalytic activity of the fabricated $\text{Ni}_{0.77}/\text{Co}_{0.23}$ -BTC BMOF was evaluated in a one-pot four-component reaction

of dimedone, aromatic aldehyde, 4-hydroxycoumarin, and ammonium acetate for the synthesis of chromeno[4,3-*b*]quinolone derivatives. To find the optimal reaction conditions, the reaction of dimedone, benzaldehyde, 4-hydroxycoumarin, and ammonium acetate was selected as a model reaction, and different factors affecting the reaction performance were optimized. Various amounts of the catalyst (0–10 mg) and different solvents, such as MeOH, EtOH, THF, CHCl_3 , and CH_2Cl_2 , were investigated for the model of the four-component reaction of dimedone, benzaldehyde, 4-hydroxycoumarin, and ammonium acetate. The optimization results are

TABLE 2 Influence of solvents and catalyst concentration on the synthesis of **4a**^a

| Entry | Catalyst | Catalyst loading (mg) | Solvent | Yield (%) |
|-------|--|-----------------------|---------------------------------|-----------|
| 1 | Ni _{0.77} /Co _{0.23} -BTC BMOF | — | EtOH | None |
| 2 | Ni _{0.77} /Co _{0.23} -BTC BMOF | 10 | EtOH | 62 |
| 3 | Ni _{0.77} /Co _{0.23} -BTC BMOF | 10 | MeOH | 58 |
| 4 | Ni _{0.77} /Co _{0.23} -BTC BMOF | 10 | Et ₂ O | 37 |
| 5 | Ni _{0.77} /Co _{0.23} -BTC BMOF | 10 | H ₂ O | 55 |
| 6 | Ni _{0.77} /Co _{0.23} -BTC BMOF | 10 | H ₂ O, EtOH | 70 |
| 7 | Ni _{0.77} /Co _{0.23} -BTC BMOF | 10 | Solvent free | 91 |
| 8 | Ni _{0.77} /Co _{0.23} -BTC BMOF | 10 | CHCl ₃ | 30 |
| 9 | Ni _{0.77} /Co _{0.23} -BTC BMOF | 10 | CH ₂ Cl ₂ | 49 |
| 10 | Ni _{0.77} /Co _{0.23} -BTC BMOF | 10 | THF | 40 |
| 11 | Ni-BTC | 10 | Solvent free | 81 |
| 12 | Co-BTC | 10 | Solvent free | 77 |
| 13 | Ni(NO ₃) ₂ | 10 | Solvent free | 42 |
| 14 | Co(NO ₃) ₂ | 10 | Solvent free | 37 |

^aThe reaction was carried out using 4-chlorobenzaldehyd (1.0 mmol), dimedone (1.0 mmol), 4-hydroxycoumarin (1.0 mmol), ammonium acetate (1.5 mmol), and 10-mg catalyst at room temperature under solvent-free condition.

TABLE 3 Synthesis of chromeno[4,3-*b*]quinolone derivatives catalyzed by Ce_{0.47}/Ni_{0.53}-BTC^a

| Entry | Substrate | Product | M.p (°C) | Yield (%) |
|-------|-----------------------------|-----------|-------------------------|-----------|
| 1 | 2-methoxyphenylbenzaldehyde | 5a | 160–162 ^[53] | 93 |
| 2 | 3-nitrobenzaldehyde | 5b | 137–139 ^[53] | 88 |
| 3 | 4-chlorophenyl | 5c | 183–184 ^[54] | 91 |
| 4 | 3-chlorobenzaldehyde | 5d | 190–192 ^[53] | 87 |
| 5 | 3-hydroxybenzaldehyde | 5e | 179–181 ^[53] | 90 |
| 6 | 4-nitrobenzaldehyde | 5f | 279–281 ^[55] | 93 |
| 7 | 4-methoxyphenylbenzaldehyde | 5g | 261–263 ^[53] | 92 |
| 8 | 2-methoxyphenylbenzaldehyde | 5h | 301–303 ^[53] | 85 |
| 9 | 3,4,5-trimethoxyphenyl | 5i | 302–303 ^[52] | 91 |
| 10 | 2-hydroxybenzaldehyde | 5j | 290–292 ^[52] | 89 |
| 11 | Thiophene-2-carbaldehyde | 5k | 237–239 | 90 |

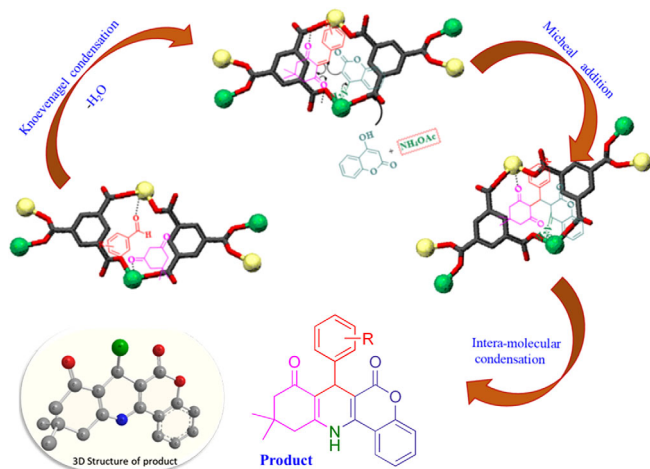
^aReaction conditions: aldehyde (1.0 mmol), dimedone (1 mmol), 4-hydroxycoumarin (1 mmol), ammonium acetate (1.5 mmol) and 10 mg catalyst, solvent-free at room temperature.

presented in Table 2. It can be observed that the catalytic activity was examined for different amounts of catalyst

under solvent-free condition (Entries 1–5). When the reaction was run without any catalyst, no product was

obtained (Entry 1). This observation proves that the presence of the $\text{Ni}_{0.77}/\text{Co}_{0.23}$ -BTC BMOF catalyst is essential for the reaction performance. The yield of the product was increased by increasing the amount of catalyst. Hence, the best yield of the product was obtained in the presence of 10 mg $\text{Ni}_{0.77}/\text{Co}_{0.23}$ -BTC, and this weight was selected for the investigation of solvent effect (Entries 6–12). It should be noted that increasing the amount of the catalyst to values greater than 10 mg did not raise the yield of the reaction. According to the yield percentages of the product, which were obtained from various solvents, the best yield was achieved in the solvent-free condition (Entry 4). Performing the reaction in different temperatures did not affect the yield of the product. In addition, the efficiency of the $\text{Ni}_{0.77}/\text{Co}_{0.23}$ -BTC catalyst was compared to other catalysts. For this purpose, the reaction was performed in the presence of other catalytic agents, including Ni-BTC, Co-BTC, $\text{Ni}(\text{NO}_3)_2$, and $\text{Co}(\text{NO}_3)_2$. The results showed that the $\text{Ni}_{0.77}/\text{Co}_{0.23}$ -BTC catalyst is the most efficient catalyst for the reaction performance. Therefore, 10 mg of the catalyst was selected as the optimal reaction conditions at room temperature under solvent-free condition.

Considering the efficiency of the above reaction protocol, a novel four-component and one-pot synthesis was designed with various functionalized aromatic aldehydes. The results are shown in Table 3. The compound structures were fully characterized by ^1H , ^{13}C NMR, FT-IR, mass spectroscopy, elemental analysis, and melting point. It can be observed that several aldehydes were used in the reaction conditions, and all of them gave the desired products in good isolated yields.



SCHEME 2 The proposed mechanism for the reaction of four components in the presence of $\text{Ni}_{0.77}/\text{Co}_{0.23}$ -BTC

With these outstanding results in hand, the mechanism of the reaction was proposed. The mechanism involves Knoevenagel condensation, Michael addition, and intramolecular cyclization.^[43] The proposed mechanism for the four-component reaction of dimedone, aromatic aldehyde, 4-hydroxycoumarin, and ammonium acetate in the presence of $\text{Ni}_{0.77}/\text{Co}_{0.23}$ -BTC is presented in Scheme 2. According to the suggested mechanism, the bimetallic centers act as the catalyst of the reaction. At the beginning of the reaction, the carbonyl groups of dimedone and aldehyde could be activated by the mentioned active sites. A Knoevenagel reaction takes place between dimedone and aldehyde, and by removing one water molecule, the 2-benzylidene-5, 5-dimethylcyclohexane-1, 3-dione intermediate is formed. 4-Hydroxycoumarin is separately reacted with ammonium acetate and forms 4-aminooumarine. In the next step of the reaction mechanism, the $\text{Ni}_{0.77}/\text{Co}_{0.23}$ -BTC-catalyzed Michael-type addition reaction of 2-benzylidene-5, 5-dimethylcyclohexane-1,3-dione, and 4-aminooumarine leads to the formation of 2-((4-imino-2-oxochroman-3-yl)(phenyl)methyl)-5,5-dimethylcyclohexane-1,3-dione intermediate. This intermediate then converts to the desired product through an intramolecular condensation.

2.3 | Reusability of the catalyst

A great advantage of the $\text{Ni}_{0.77}/\text{Co}_{0.23}$ -BTC catalyst is its reusability. The reusability of the catalyst was screened by the separation of the catalyst from the reaction mixture

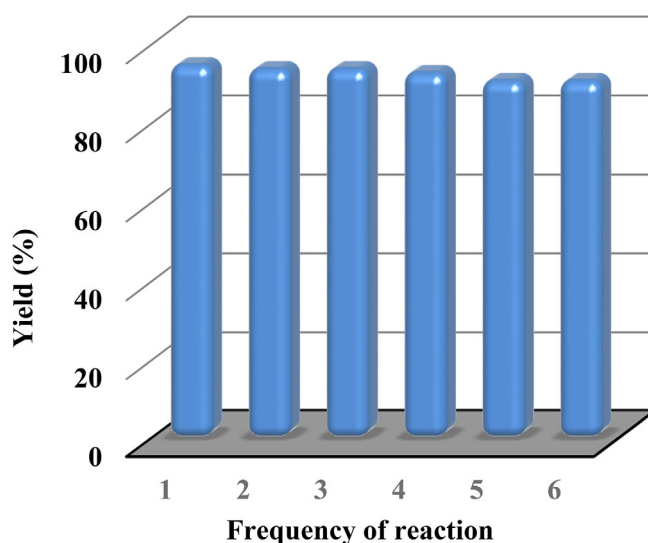


FIGURE 3 Reusability of $\text{Ni}_{0.77}/\text{Co}_{0.23}$ -BTC BMOF catalyst after six sequential runs

after the reaction was completed and used in the next reaction. This recovery was repeated six times. The results are presented in Figure 3. It can be observed that the catalyst was active after six sequential runs, and no decrease in the catalytic activity of $\text{Ni}_{0.77}/\text{Co}_{0.23}\text{-BTC}$ was observed.

For studying the stability of the catalyst under the reaction conditions, the $\text{Ni}_{0.77}/\text{Co}_{0.23}\text{-BTC}$ catalyst was characterized by the XRD method after the fifth recovery. For this purpose, the catalyst was used in sequential reactions. After

the fifth cycle, the $\text{Ni}_{0.77}/\text{Co}_{0.23}\text{-BTC}$ catalyst was separated from the reaction mixture, washed with ethanol, and dried in a vacuum oven. Then, the crystalline structure of the $\text{Ni}_{0.77}/\text{Co}_{0.23}\text{-BTC}$ catalyst was studied by the XRD method. The result is presented in Figure 4. It could be seen that the structure of the catalyst remained unchanged during the reaction, and a similar XRD pattern is observed.

3 | EXPERIMENTAL

3.1 | Chemicals and materials

All precursors including $\text{Ni}(\text{NO}_3)_2 \cdot 6\text{H}_2\text{O}$, $\text{Co}(\text{NO}_3)_2 \cdot 6\text{H}_2\text{O}$, ethanol (96%), sodium nitrate (NaNO_3 , 99%), and benzene-1,3,5-tricarboxylic acid (H_3BTC , 95%) were purchased from Sigma-Aldrich and used as received. All of solutions were made with Milli-Q water in the experimental sections.

3.2 | Instruments

The size and morphology of the synthesized BMOF were observed through field-emission scanning electron microscopy (FE-SEM, Model TE-SCAN MIRA3, operating

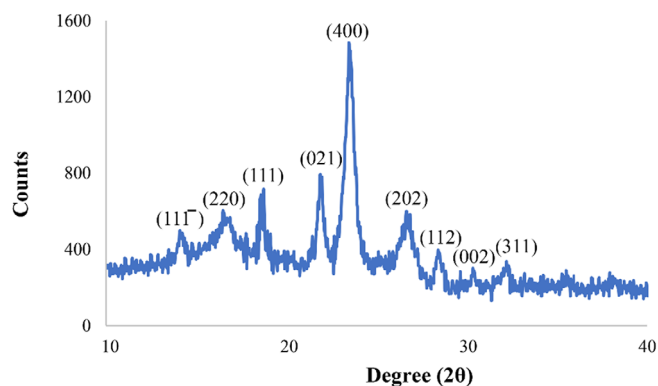
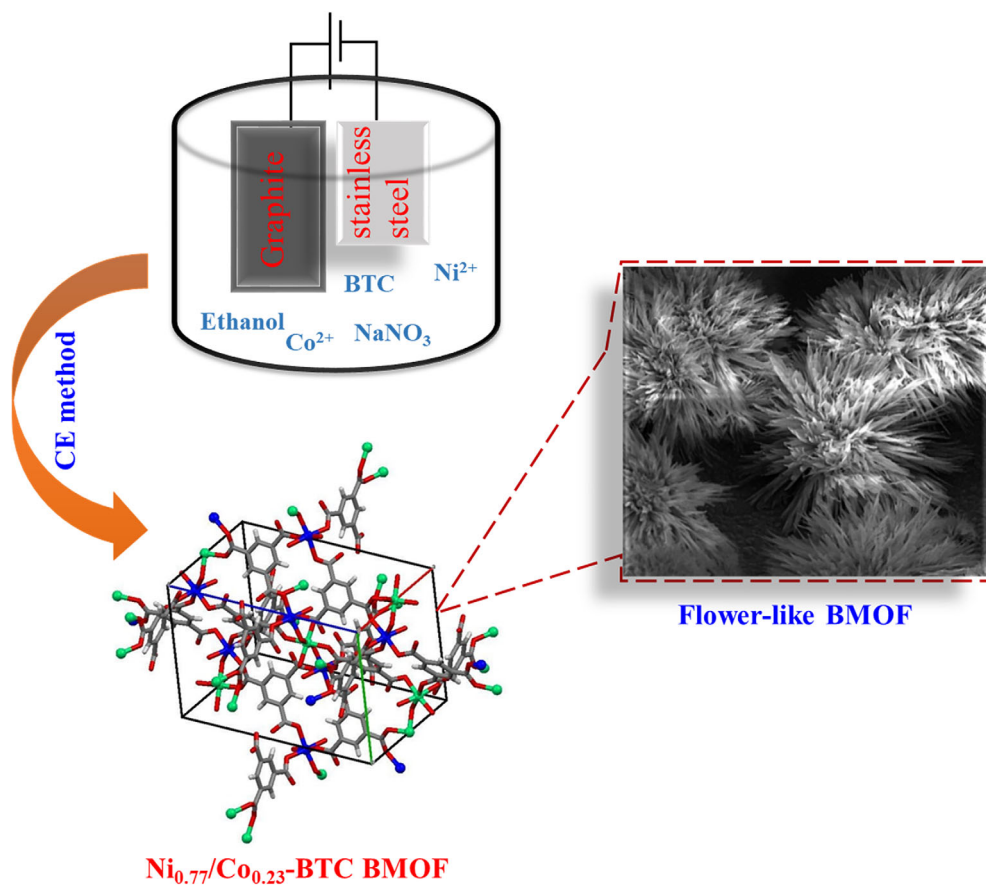


FIGURE 4 XRD pattern of $\text{Ni}_{0.77}/\text{Co}_{0.23}\text{-BTC}$ BMOF catalyst after fifth cycle of recovery



SCHEME 3 The general route of CE of 3D flower-like $\text{Ni}_{0.77}/\text{Co}_{0.23}\text{-BTC}$ BMOF

voltage 30 kV), and the elemental data were collected using energy-dispersive spectroscopy (EDS) on this system. The crystal phase and structure of the sample were determined by XRD, using a model Phillips PW-1800 diffractometer with Cu K α radiation ($\lambda = 1.5406 \text{ \AA}$). The FT-IR spectrum of the sample was acquired using the Bruker Vector 22 IR instrument.

3.3 | Electrochemical preparation of flower-like Ni_{0.77}/Co_{0.23}-BTC BMOF

The CE method was implemented between two electrodes in constant current conditions. To set up the electrochemical cell, a cell composed of a graphite sheet (as anode, size = 7 cm \times 7 cm) and stainless steel sheet (as cathode, size = 5 cm \times 5 cm) was used. To obtain deposit on both sides of the cathode electrode, the steel cathode was centered between two graphite anodes. The electrolyte bath was prepared by dissolving 150 mg of nickel nitrate, 50 mg of cobalt nitrate, 100 mg of BTC, and 50 mg NaNO₃ in 200 ml of ethanol. For electrodeposition of Ni/Co-BTC, a cathodic current density of 10 mA/cm² was applied for 30 min to the above-mentioned electrochemical system. It was observed that a violaceous deposit was formed on both sides of stainless steel cathode at the end of the deposition time. After this step, the steel cathode was removed from the electrochemical bath and washed several times with ethanol. Then, the deposit was separated from the cathode surface and dried at 70°C for 2 hr. The obtained powder was the final product and named flower-like Ni_{0.77}/Co_{0.23}-BTC BMOF. The general route of CE of the 3D flower-like Ni_{0.77}/Co_{0.23}-BTC BMOF is illustrated in Scheme 3.

3.4 | General procedure for the synthesis of compounds of 5a-5j

A mixture of dimedone (1 mmol), aromatic aldehyde (1 mmol), hydroxycoumarin (1 mmol), and ammonium acetate (1.5 mmol) was mixed together in a round-bottomed flask, and the flower-like Ni_{0.77}/Co_{0.23}-BTC BMOF (10 mg) was added. The mixture was stirred under solvent-free condition at room temperature for 45 min. The reaction evolution was controlled by the TLC (hexane: ethyl acetate, 4:1). Then, hot ethanol was added to the reaction mixture and stirred at room temperature for 15 min. The catalyst was centrifuged and separated. The solution was placed in a cooling bath until a solid white product was obtained. Then, it was recrystallized with ethanol.

3.5 | Spectral data for the selected products

7-(3-methoxyphenyl)-10,10-dimethyl-7,10,11,12-tetrahydro-6H-chromeno[4,3-b]quinoline-6,8(9H)-dione

Solid white, M.p: 271–273°C; ¹H-NMR (250 MHz, DMSO-d₆): $\delta = 9.69$ (s, NH), 8.27 (1H, d, Ar-H, J = 7.5 Hz), 7.61 (1H, t, Ar-H, J = 7.5 Hz), 7.39 (2H, q, Ar-H, J = 11.5 Hz), 7.10 (1H, t, Ar-H, J = 7.75 Hz), 6.68 (2H, d, Ar-H, J = 8.75 Hz), 6.67 (1H, d, Ar-H, J = 7 Hz), 3.64 (3H, s, CH₃), 4.91 (1H, s, CH), 2.63 (2H, s, CH₂), 2.26 (1H, d, CH₂, J = 32.0 Hz), 2.05 (1H, d, CH₂, J = 32.0 Hz), 1.19 (3H, s, CH₃), 0.85 (3H, s, CH₃) ppm; ¹³C NMR (60 MHz, DMSO-d₆): $\delta = 196.1, 161.7, 160.4, 153.5, 151.2, 148.6, 143.6, 133.4, 130.5, 125.5, 124.4, 121.4, 118.3, 115.5, 114.5, 112.4, 112.1, 103.1, 56.3, 51.6, 41.9, 41.6, 41.3, 40.9, 40.6, 40.3, 39.9, 35.7, 33.6, 30.5, 28.0$ ppm; IR (KBr) cm⁻¹: 3,220.92, 2,945.79, 1,666.13, 1,656.08, 1,644.64, 1,605.93, 1,581.90, 1,571.65, 1,508.17, 1,473.67, 1,305.49, 1,305.49, 1,261.02, 1,238.73, 1,196.02, 1,158.72, 1,045.81, 766.42, 752.20, 691.92; Mass (Mz+): 401; Anal. Calcd for C₂₅H₂₃NO₄: C, 74.80; H, 5.77; N, 3.49, Found: C, 74.76; H, 5.79; N, 3.54.

7-(3-nitrophenyl)-10,10-dimethyl-7,10,11,12-tetrahydro-6H-chromeno[4,3-b]quinoline-6,8(9H)-dione

Solid white, M.p: 289–296°C. ¹H-NMR (250 MHz, DMSO-d₆): $\delta = 9.80$ (s, NH), 8.29 (1H, d, Ar-H, J = 6.5 Hz), 8.02 (1H, s, Ar-H), 7.96 (2H, d, Ar-H, J = 7.25 Hz), 7.677–7.324 (5H, m, Ar-H), 5.02 (1H, s, CH), 2.66 (2H, s, CH₂), 2.26 (1H, d, CH₂, J = 34 Hz), 20.5 (1H, d, CH₂, J = 34 Hz), 1.16 (3H, s, CH₃), 0.97 (3H, s, CH₃) ppm; ¹³C NMR (60 MHz, DMSO-d₆): $\delta = 161.7, 153.6, 151.8, 149.2, 149.0, 144.0, 136.1, 133.7, 131.0, 125.6, 124.6, 123.8, 122.8, 118.4, 114.3, 111.5, 102.4, 51.4, 42.0, 41.6, 41.3, 41.0, 40.6, 40.3, 40.0, 36.5, 33.7, 30.5, 27.9$ ppm; IR (KBr) cm⁻¹: 3,222.34, 3,090.63, 2,969.76, 2,941.76, 1,654.97, 1,605.42, 1,570.86, 1,524.30, 1,507.96, 1,470.96, 1,365.56, 1,344.38, 1,312.96, 1,299.38, 1,236.01, 1,191.27, 1,161.68, 1,150.36, 1,124.30, 1,084.31, 1,044.74, 1,026.52, 6,885.01, 897.00, 863.42, 809.57, 784.81, 761.62, 747.18, 737.84, 720.09, 710.81, 667.28, 652.60, 626.88, 616.51, 511.37, 496.89; Mass (Mz+): 416; Anal. Calcd for C₂₄H₂₀N₂O₅: C, 69.22; H, 6.73; N, 6.73, Found: C, 69.27; H, 6.69; N, 6.71.

7-(4-chlorophenyl)-10,10-dimethyl-7,10,11,12-tetrahydro-6H-chromeno[4,3-b]quinoline-6,8(9H)-dione

Solid white, M.p: 256–259°C. ¹H-NMR (250 MHz, DMSO-d₆): $\delta = 9.70$ (s, NH), 8.27 (1H, d, Ar-H, J = 6.5 Hz), 7.59

(1H, d, Ar-H, J = 6.5 Hz), 7.407–7.224 (6H, m, Ar-H), 4.90 (1H, s, CH), 2.62 (2H, s, CH₂), 2.24 (1H, d, CH₂, J = 34 Hz), 20.4 (1H, d, CH₂, J = 34 Hz), 1.03 (3H, s, CH₃)–0.89 (3H, 3, CH₃) ppm. ¹³C NMR (60 MHz, DMSO-d₆): δ = 196.2, 161.7, 153.5, 151.3, 146.2, 143.7, 133.5, 132.2, 131.1, 129.4, 125.5, 124.5, 118.3, 114.4, 111.9, 102.8, 51.5, 41.9, 41.6, 41.2, 40.9, 40.6, 40.2, 39.9, 35.7, 33.6, 30.5, 28.0 ppm; IR (KBr) cm⁻¹: 3,308.66, 2,959.95, 2,933.95, 1,682.68, 1,670.76, 1,645.25, 1,605.98, 1,568.74, 1,505.03, 1,464.94, 1,449.09, 1,425.59, 1,362.49, 1,362.49, 1,312.63, 1,235.63, 1,235.95, 1,194.67, 1,159.55, 1,147.33, 1,089.62, 1,041.56, 1,014.03, 874.87, 851.79, 830.13, 758.58, 733.91, 712.93, 650.59, 585.58, 571.41, 539.79, 461.42, 432.13, 417.00; Anal. Calcd for C₂₄H₂₀ClNO₃: C, 71.02; H, 4.97; N, 3.45, Found: C, 71.06; H, 4.99; N, 3.41.

4 | CONCLUSIONS

A simple, convenient, and safe synthetic methodology has been introduced for the synthesis of chromeno[4,3-*b*]quinolone derivatives at room temperature under solvent-free conditions. The method is based on the use of the Ni_{0.77}/Co_{0.23}-BTC BMOF as a heterogeneous catalyst for the one-pot multicomponent reaction of dimedone, aromatic aldehyde, 4-hydroxycoumarin, and ammonium acetate. The presented 3D flower-like Ni_{0.77}/Co_{0.23}-BTC BMOF was synthesized via the CE method, which provides many advantages such as milder synthesis conditions, shorter reaction times, and the ability to control the rate of synthesis. The catalytic activity of the prepared BMOF in the synthesis of chromeno[4,3-*b*]quinolone derivatives was very good, and the starting materials gave the desired products in high isolated yields. The simplicity of the BMOF synthesis and mild reaction conditions will also make this synthetic protocol marvelous and beneficial at an industrial scale. The catalyst showed very good reusability in the reaction conditions, and no loss in the activity of the catalyst was observed after six sequential reactions.

ACKNOWLEDGMENTS

The authors thank the University Research Council for financial support of this work.

REFERENCES

- [1] M. R. Ryder, J.-C. Tan, *Mater. Sci. Technol.* **2014**, *30*, 1598.
- [2] R. R. Salunkhe, Y. Kamachi, N. L. Torad, S. M. Hwang, Z. Sun, S. X. Dou, J. H. Kim, Y. Yamauchi, *J. Mater. Chem. A* **2014**, *2*, 19848.
- [3] X.-Y. Hou, X. Wang, S.-N. Li, Y.-C. Jiang, M.-C. Hu, Q.-G. Zhai, *Cryst. Growth Des.* **2017**, *17*, 3229.
- [4] V. Pezeshkpour, S. A. Khosravani, M. Ghaedi, K. Dashtian, F. Zare, A. Sharifi, R. Jannesar, M. Zoladl, *Ultrason. Sonochem.* **2018**, *40*, 1031.
- [5] O. Abuzalat, D. Wong, M. Elsayed, S. Park, S. Kim, *Ultrason. Sonochem.* **2018**, *45*, 180.
- [6] H. L. Nguyen, T. T. Vu, D.-K. Nguyen, C. A. Trickett, T. L. Doan, C. S. Diercks, V. Q. Nguyen, K. E. Cordova, *Commun. Chem.* **2018**, *1*, 70.
- [7] C. Chen, X. Feng, Q. Zhu, R. Dong, R. Yang, Y. Cheng, C. He, *Inorg. Chem.* **2019**, *58*, 2717.
- [8] S. L. Griffin, C. Wilson, R. S. Forgan, *Front. Chem.* **2019**, *7*, 36.
- [9] D. J. Bara, C. Wilson, M. Mörtel, M. M. Khusniyarov, S. Ling, B. Slater, S. Sproules, R. S. Forgan, *J. Am. Chem. Soc.* **2019**, *141*, 8346.
- [10] J. W. Maina, C. P. Gonzalo, A. Merenda, L. Kong, J. A. Schütz, L. F. Dumée, *Appl. Surf. Sci.* **2018**, *427*, 401.
- [11] L. Li, S. Shen, J. Su, W. Ai, Y. Bai, H. Liu, *Anal. Bioanal. Chem.* **2019**, *18*, 4213.
- [12] R. Ye, M. Ni, Y. Xu, H. Chen, S. Li, *RSC Adv.* **2018**, *8*, 26237.
- [13] Y. Liu, L. Wang, H. Feng, X. Ren, J. Ji, F. Bai, H. Fan, *Nano Lett.* **2019**, *19*, 2614.
- [14] A. Chatterjee, X. Hu, F. L.-Y. Lam, *Appl. Catal. A Gen.* **2018**, *566*, 130.
- [15] O. J. de Lima Neto, A. C. de Oliveira Frós, B. S. Barros, A. F. de Farias Monteiro, J. Kulesza, *New J. Chem.* **2019**, *14*, 5518.
- [16] L. Chen, J. Du, W. Zhou, H. Shen, L. Tan, C. Zhou, L. Dong, *Chem. Asian J.* **2020**, *15*, 3421.
- [17] W. Li, S. Watzele, H. A. El-Sayed, Y. Liang, G. Kieslich, A. S. Bandarenka, K. Rodewald, B. Rieger, R. A. Fischer, *J. Am. Chem. Soc.* **2019**, *141*, 5926.
- [18] W. Li, S. Xue, S. Watzele, S. Hou, J. Fichtner, A. L. Semrau, L. Zhou, A. Welle, A. S. Bandarenka, R. A. Fischer, *Angew. Chem. Int. Ed.* **2020**, *59*, 5837.
- [19] J. Yang, P. Xiong, C. Zheng, H. Qiu, M. Wei, *J. Mater. Chem. A* **2014**, *2*, 16640.
- [20] X. Xu, R. Cao, S. Jeong, J. Cho, *Nano Lett.* **2012**, *12*, 4988.
- [21] H. Gholipour-Ranjbar, M. Soleimani, H. R. Naderi, *New J. Chem.* **2016**, *40*, 9187.
- [22] R. Grunker, V. Bon, A. Heerwig, N. Klein, P. Müller, U. Stoeck, I. A. Baburin, U. Mueller, I. Senkovska, S. Kaskel, *Chem. A Eur. J.* **2012**, *18*, 13299.
- [23] W. Yin, C.-A. Tao, F. Wang, J. Huang, T. Qu, J. Wang, *Sci. China Mater.* **2018**, *61*, 391.
- [24] X. Song, M. Oh, M. S. Lah, *Inorg. Chem.* **2013**, *52*, 10869.
- [25] A. Arnanz, M. Pintado-Sierra, A. Corma, M. Iglesias, F. Sánchez, *Adv. Synth. Catal.* **2012**, *354*, 1347.
- [26] M. Castellano, N. Moliner, J. Cano, F. Lloret, *Polyhedron* **2019**, *170*, 7.
- [27] X. Lin, E. Ning, X. Li, Q. Li, *Chin. Chem. Lett.* **2019**, *31*, 813.
- [28] L. Yu, Q. Zheng, D. Wu, Y. Xiao, *Sensor. Actuat. B Chem.* **2019**, *294*, 199.
- [29] Z. Li, J. Cui, Y. Liu, J. Li, K. Liu, M. Shao, *ACS Appl. Mater. Interfaces* **2018**, *10*, 34494.
- [30] M. Aghazadeh, M. R. Ganjali, *Ceram. Int.* **2018**, *44*, 520.
- [31] M. Aghazadeh, I. Karimzadeh, M. R. Ganjali, *J. Mater. Sci. Mater. Electron.* **2017**, *28*, 13532.
- [32] M. Aghazadeh, *Mater. Lett.* **2018**, *211*, 225.
- [33] M. Aghazadeh, M. R. Ganjali, *J. Mater. Sci. Mater. Electron.* **2018**, *29*, 2291.
- [34] Y.-S. Kang, Y. Lu, K. Chen, Y. Zhao, P. Wang, W.-Y. Sun Eds., *Coord. Chem. Rev.* **2019**, *378*, 262.

- [35] J.-S. M. Lee, Y.-I. Fujiwara, S. Kitagawa, S. Horike, *Chem. Mater.* **2019**, *31*, 4205.
- [36] Y. B. Huang, Q. Wang, J. Liang, X. Wang, R. Cao, *J. Am. Chem. Soc.* **2016**, *138*, 10104.
- [37] J. Liang, R. P. Chen, X. Y. Wang, T. T. Liu, X. S. Wang, Y. B. Huang, R. Cao, *Chem. Sci.* **2017**, *8*, 1570.
- [38] S. Chaemchuen, X. Xiao, M. Ghadamyari, B. Mousavi, N. Klomkliang, Y. Yuan, F. Verpoort, *J. Catal.* **2019**, *370*, 38.
- [39] M. Yadollahi, H. Hamadi, V. Nobakht, *Appl. Organomet. Chem.* **2019**, *33*, e4819.
- [40] D. Sun, W. Liu, M. Qiu, Y. Zhang, Z. Li, *Chem. Commun.* **2015**, *51*, 2056.
- [41] R. Sun, B. Liu, B. G. Li, S. Jie, *ChemCatChem* **2016**, *8*, 3261.
- [42] M. Almasi, V. Zelenak, M. Opanasenko, I. Cisarova, *Catal. Today* **2015**, *243*, 184.
- [43] Y. Huang, Y. Zhang, X. Chen, D. Wu, Z. Yi, R. Cao, *Chem. Commun.* **2014**, *50*, 10115.
- [44] S. T. Xiao, C. T. Ma, J. Q. Di, Z. H. Zhang, *New J. Chem.* **2020**, *44*, 8614.
- [45] G. Gao, J. Q. Di, H. Y. Zhang, L. P. Mo, Z. H. Zhang, *J. Catal.* **2020**, *387*, 39.
- [46] J. N. Zhang, X. H. Yang, W. J. Guo, B. Wang, Z. H. Zhang, *Synlett* **2017**, *28*, 734.
- [47] M. Sanaei, R. Fazaeli, H. Aliyan, *J. Chin. Chem. Soc.* **2019**, *66*, 1290.
- [48] H. Al-Kutubi, J. Gascon, E. J. Sudhölter, L. Rassaei, *ChemElectroChem* **2015**, *2*, 462.
- [49] S. Gao, Y. Sui, F. Wei, J. Qi, Q. Meng, Y. Ren, Y. He, *J. Colloid Interface Sci.* **2018**, *531*, 83.
- [50] T. Yang, Y. Liu, D. Yang, B. Deng, Z. Huang, C. D. Ling, H. Liu, G. Wang, Z. Guo, R. Zheng, *Energy Storage Mater.* **2019**, *17*, 374.
- [51] M. S. Rahmanifar, H. Hesari, A. Noori, M. Y. Masoomi, A. Morsali, M. F. Mousavi, *Electrochim. Acta* **2018**, *275*, 76.
- [52] N. Ahmed, B. V. Babu, S. Singh, *Heterocycles* **2012**, *85*, 1629.
- [53] A. Yahya-Meymandi, H. Nikookar, S. Moghimi, M. Mahdavi, L. Firoozpour, A. Asadipour, P. R. Ranjbar, A. Foroumadi, *J. Iran. Chem. Soc.* **2017**, *14*, 771.
- [54] S. Bahadorikhalili, S. Mohammadi, M. Asadi, M. Barazandeh, M. Mahdavi, *J. Chin. Chem. Soc.* **2020**, *67*, 160.
- [55] S. Paul, A. R. Das, *Tetrahedron Lett.* **2012**, *53*, 2206.

SUPPORTING INFORMATION

Additional supporting information may be found online in the Supporting Information section at the end of this article.

How to cite this article: Sayahi MH, Ghomi M, Hamad SM, et al. Electrochemical synthesis of three-dimensional flower-like Ni/Co-BTC bimetallic organic framework as heterogeneous catalyst for solvent-free and green synthesis of substituted chromeno[4,3-*b*]quinolones. *J Chin Chem Soc.* 2020;1–10. <https://doi.org/10.1002/jccs.202000314>